

# A *cis*-Divacant Octahedral and Mononuclear Iron(IV) Imide\*\*

Keith Searles, Skye Fortier,\* Marat M. Khusniyarov, Patrick J. Carroll, Jörg Sutter, Karsten Meyer,\* Daniel J. Mindiola,\* and Kenneth G. Caulton\*

Dedicated to Professor T. Don Tilley on the occasion of his 60<sup>th</sup> birthday

**Abstract:** A rare, low-spin Fe<sup>IV</sup> imide complex [(pyrr<sub>2</sub>py)-Fe=NAd] (pyrr<sub>2</sub>py<sup>2-</sup> = bis(pyrr<sub>2</sub>py)pyridine; Ad = 1-adamantyl) confined to a *cis*-divacant octahedral geometry, was prepared by reduction of N<sub>3</sub>Ad by the Fe<sup>II</sup> precursor [(pyrr<sub>2</sub>py)Fe(OEt<sub>2</sub>)]. The imide complex is low-spin with temperature-independent paramagnetism. In comparison to an authentic Fe<sup>III</sup> complex, such as [(pyrr<sub>2</sub>py)FeCl], the pyrr<sub>2</sub>py<sup>2-</sup> ligand is virtually redox innocent.

It has been well-established that the catalytic cycles of many heme and non-heme iron metalloenzymes utilize transiently generated, multiply bonded, high-valent iron centers as potent oxidants.<sup>[1,2]</sup> These iron centers are principally in the +4 oxidation state, such as that found for Fe<sup>IV</sup>(oxo)(porphyrin  $\pi$ -radical cation) in Cytochrome P450. It has also been shown that the heme-containing terminal oxidase enzymes of the P450 platform can perform nitrene transfer chemistry which is thought to proceed via a putative Fe<sup>IV</sup> imide intermediate.<sup>[1b,3]</sup> Thus, the electronic and structural characterization of molecules containing Fe<sup>IV</sup>=E moieties (E = O, NR) are important for providing better insight into the active species of iron metalloenzymes and developing group-transfer catalysts.<sup>[1b,4]</sup> However, relatively few Fe<sup>IV</sup> complexes featuring terminal oxo<sup>[5]</sup> or imide<sup>[6]</sup> ligands

have been isolated in the solid-state and structurally characterized.

The support of stable Fe<sup>IV</sup>=E functionalities requires an ancillary ligand that is sufficiently electron donating and resistant to oxidative degradation, while providing a coordination geometry that minimizes filled–filled  $p\pi$ – $d\pi$  orbital repulsions<sup>[7]</sup> within the multiply bonded Fe<sup>IV</sup>=E fragment. Interestingly, of the structurally characterized Fe<sup>IV</sup> imides, only tetrahedral<sup>[6a–c]</sup> and octahedral<sup>[6d]</sup> coordination geometries are known, in part because of their low-spin nature and ligand-field stabilization energies. For example, Peters et al. and Smith and co-workers have each successfully utilized tripodal ligands with strongly electron-donating phosphine/pyrazolyl and N-heterocyclic carbene donors, respectively, to stabilize tetrahedral [LFe<sup>IV</sup>=NAd]<sup>+</sup> complexes from the one-electron oxidation of [LFe<sup>III</sup>=NAd] precursors (L = bis((di-*tert*-butylphosphino)methyl)(3,5-dimethylpyrazole)phenylborate, or tris(1-mesitylimidazol-2-ylidene)phenylborate; Ad = 1-adamantyl).<sup>[6b,c]</sup>

Recently, we reported the synthesis of a bulky bis-(pyrr<sub>2</sub>py)pyridine pincer (H<sub>2</sub>pyrr<sub>2</sub>py, Scheme 1) and its coordination chemistry with a variety of late transition metals, including Fe<sup>II</sup>.<sup>[8]</sup> Herein, we describe the synthesis of a novel Fe<sup>II</sup> complex supported by the dianionic pyrr<sub>2</sub>py pincer, namely [(pyrr<sub>2</sub>py)Fe(OEt<sub>2</sub>)], and discuss its clean and direct conversion into the Fe<sup>IV</sup> imide [(pyrr<sub>2</sub>py)Fe=NAd]. The four-coordinate Fe<sup>IV</sup> imide complex has a coordinatively

[\*] Prof. Dr. S. Fortier

Department of Chemistry, University of Texas at El Paso  
El Paso, Texas 79968 (USA)  
E-mail: asfortier@utep.edu

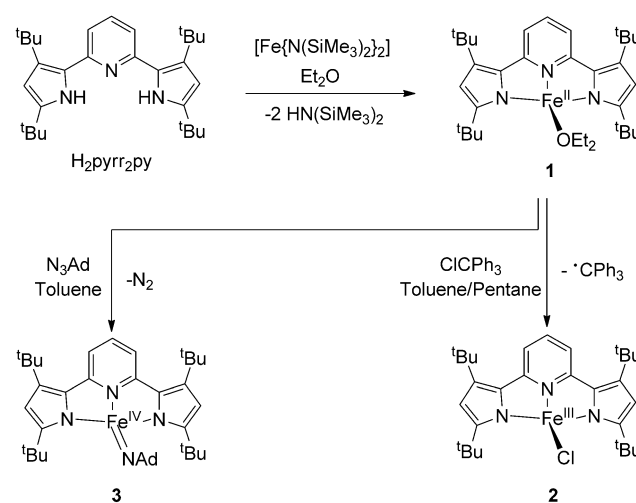
K. Searles, Dr. P. J. Carroll, Prof. Dr. D. J. Mindiola  
Department of Chemistry, University of Pennsylvania  
Philadelphia, PA 19104 (USA)  
E-mail: mindiola@sas.upenn.edu

Prof. Dr. K. G. Caulton  
Department of Chemistry and Molecular Structure Center  
Indiana University, Bloomington, IN 47505 (USA)  
E-mail: caulton@indiana.edu

Dr. M. M. Khusniyarov, Dr. J. Sutter, Prof. Dr. K. Meyer  
Department of Chemistry and Pharmacy, Inorganic Chemistry  
Friedrich-Alexander University Erlangen-Nürnberg (FAU)  
Erlangen (Germany) 91058  
E-mail: karsten.meyer@fau.de

[\*\*] This work was supported in part by the NSF ACC-F (CHE-1137284; S.F.). D.J.M. also thanks Indiana University and the University of Pennsylvania for financial support of this research. Rene Buell is thanked for preliminary experiments contributing to this work.

Supporting information for this article is available on the WWW under <http://dx.doi.org/10.1002/anie.201407156>.



**Scheme 1.** Synthesis of [(pyrr<sub>2</sub>py)Fe(OEt<sub>2</sub>)] (1), [(pyrr<sub>2</sub>py)FeCl] (2), and [(pyrr<sub>2</sub>py)Fe=NAd] (3).

unsaturated metal center, whose new and unusual geometry is best described as a *cis*-divacant octahedron. Spectroscopic, magnetic, and theoretical studies have been combined to address the unique electronic structure of this system.

Coordination of a single bis(pyrrolyl)pyridine ligand to iron was accomplished by the slow addition of one equivalent of  $\text{H}_2\text{pyrr}_2\text{py}$  to  $[\text{Fe}(\text{N}(\text{SiMe}_3)_2)_2]$  in  $\text{Et}_2\text{O}$ , which yielded a red solution after stirring for 14 hours. The mononuclear complex  $[(\text{pyrr}_2\text{py})\text{Fe}(\text{OEt}_2)]$  (**1**) was obtained in 81 % yield and crystallizes as red plates from concentrated  $\text{Et}_2\text{O}$  or pentane solutions stored at  $-35^\circ\text{C}$ . The  $^1\text{H}$  NMR spectrum of **1** recorded in  $\text{C}_6\text{D}_6$  at room temperature reveals seven broad resonance signals, ranging from  $\delta = -2.9$  ppm to 120.5 ppm, attributable to protons of a paramagnetic complex, which are consistent with a  $\text{C}_s$  symmetric structure in solution. Solution magnetic susceptibility measurements of **1**, determined by the Evans method in  $\text{C}_6\text{D}_6$  at room temperature, indicate a magnetic susceptibility value of  $5.2 \mu_{\text{B}}$ , which is only slightly higher than the calculated spin-only value of  $4.9 \mu_{\text{B}}$  for a high-spin  $\text{Fe}^{\text{II}}$  complex ( $S = 2$ ). Variable-temperature SQUID magnetization measurements also indicate a high-spin  $\text{Fe}^{\text{II}}$  complex, which confirms a negligibly temperature-dependent effective magnetic moment ( $\mu_{\text{eff}}$ ) ranging from  $5.09$  to  $5.25 \mu_{\text{B}}$  over the temperature range  $30$ – $300$  K (dc mode).<sup>[9]</sup>

The solid-state molecular structure of **1** (Figure 1a) reveals a four-coordinate iron center bound by one  $\text{Et}_2\text{O}$  molecule and the tridentate  $\text{pyrr}_2\text{py}$  ligand in a meridional configuration. The  $\text{Fe}-\text{N}_{\text{py}}$  ( $\text{Fe1}-\text{N1} = 2.021(2)$  Å) and  $\text{Fe}-\text{N}_{\text{pyrr}}$  ( $\text{Fe1}-\text{N2} = 1.987(1)$  Å) distances are unexceptional and comparable to those of recently reported  $[(\text{Hpyrr}_2\text{py})_2\text{Fe}]$  (e.g.  $\text{Fe}-\text{N}_{\text{py}} = 2.077(2)$  Å,  $\text{Fe}-\text{N}_{\text{pyrr}} = 2.012(2)$  Å).<sup>[8]</sup> Notably, the iron center in **1** exhibits a non-planar coordination geometry, with a deviation of  $0.57$  Å from the plane defined by the three  $\text{pyrr}_2\text{py}$  nitrogens, and with the coordinated  $\text{Et}_2\text{O}$  found *cis* ( $\text{N1}-\text{Fe1}-\text{O1} = 102.37(8)^\circ$ ,  $\text{N2}-\text{Fe1}-\text{O1} = 106.03(4)^\circ$ ) to the  $\text{pyrr}_2\text{py}$  ligand. The most valid geometric description of **1** is between trigonal pyramidal and *cis*-divacant octahedral ( $\tau_4 = 0.80$ ),<sup>[10]</sup> reminiscent of that found for the  $\text{Zn}^{\text{II}}$  analogue  $[(\text{pyrr}_2\text{py})\text{Zn}(\text{DMAP})]$  ( $\text{DMAP} = \textit{para}$ -(dimethylamino)-pyridine).<sup>[8]</sup> A space-filling model<sup>[9]</sup> of **1** suggests that the *tert*-butyl groups of the pyrrole  $\alpha$ -carbons effectively block the site *trans* to the pyridyl nitrogen, preventing adoption of a square-planar geometry.

Intrigued by the idea of stabilizing high-valent iron complexes, we subsequently investigated the one- and two-electron chemical oxidations of complex **1**. Single-electron oxidation was accomplished by the reaction of  $\text{ClCPh}_3$  (1 equiv) with **1** in a toluene/pentane mixture to afford the mononuclear  $\text{Fe}^{\text{III}}$  complex  $[(\text{pyrr}_2\text{py})\text{FeCl}]$  (**2**) in 72 % yield as a dark red/brown microcrystalline material (Scheme 1). Upon separation of Gombert's radical and dimer, the  $^1\text{H}$  NMR spectrum of **2**, recorded in  $\text{C}_6\text{D}_6$  at room temperature, displays five broad resonance signals in the range  $\delta = 10.4$ – $143.3$  ppm, which is consistent with loss of  $\text{Et}_2\text{O}$  from the molecule and the preservation of the  $\text{C}_s$  symmetry. X-ray diffraction studies were performed on red single crystals, grown by layering a concentrated toluene solution of **2** with pentane stored at  $-35^\circ\text{C}$ . The solid-state structure of **2** (Figure 1b) shows that the molecule adopts a geometry between trigonal pyramidal and *cis*-divacant octahedral ( $\tau_4 = 0.73$ )<sup>[10]</sup> where the  $\text{Fe}-\text{N}_{\text{py}}$  ( $\text{Fe1}-\text{N2} = 1.981(2)$  Å) and  $\text{Fe}-\text{N}_{\text{pyrr}}$  ( $\text{Fe1}-\text{N1} = 1.991(2)$  Å) distances are comparable to that of the  $\text{Fe}^{\text{II}}$  precursor. Similar to **2**, the iron center is positioned  $0.62$  Å above the plane defined by the three  $\text{pyrr}_2\text{py}$  nitrogens. It is noteworthy that the  $\text{N}_{\text{py}}-\text{Fe}-\text{Cl}$  angle ( $\text{N2}-\text{Fe1}-\text{Cl1} = 115.02(8)^\circ$ ) is  $9^\circ$  more obtuse when compared to the  $\text{N}_{\text{py}}-\text{Fe}-\text{OEt}_2$  angle ( $\text{N1}-\text{Fe1}-\text{O1} = 102.37(8)^\circ$ ) of complex **1**. Variable-temperature SQUID magnetization measurements performed on **2** indicate a high-spin  $\text{Fe}^{\text{III}}$  center ( $S = 5/2$ ), which also shows a negligibly temperature-dependent  $\mu_{\text{eff}}$  value, ranging from  $5.83$  to  $5.73 \mu_{\text{B}}$  over the temperature range  $30$ – $300$  K (dc mode).<sup>[9]</sup>

We subsequently investigated the two-electron oxidation of **1** with an alkyl azide in attempts to generate an  $\text{Fe}^{\text{IV}}$  imide complex. Treatment of **1** with 1-adamantyl azide ( $\text{N}_3\text{Ad}$ ; 1 equiv) at room temperature, in either toluene or  $\text{Et}_2\text{O}$ , results in the slow formation of a dark red/purple solution over the course of 13 hours from which the product can be isolated in 96 % yield. Single-crystal X-ray diffraction studies performed on a dark-red crystal confirmed the formation of the expected  $[(\text{pyrr}_2\text{py})\text{Fe}=\text{NAd}]$  (**3**) (Figure 1c). Chirik et al. have recently reported a series of Fe imide complexes,<sup>[11]</sup> which deviate from idealized square-planar geometry. However, the overall *cis*-divacant geometry ( $\tau_4 = 0.68$ )<sup>[10]</sup> and oxidation state of complex **3** represents an entirely unprecedented coordination environment in Fe imide chemistry. The imide is positioned *cis* ( $\text{N1}-\text{Fe1}-\text{N3} =$

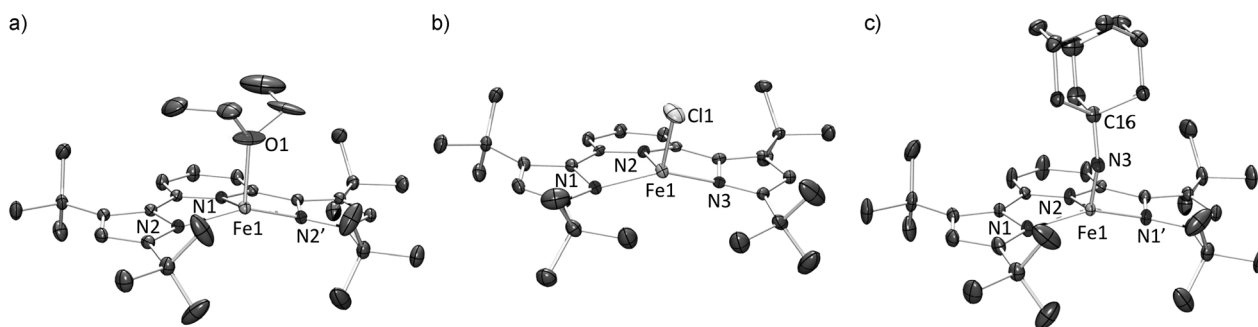


**Figure 1.** ORTEP drawings of a)  $[(\text{pyrr}_2\text{py})\text{Fe}(\text{OEt}_2)]$  (**1**), b)  $[(\text{pyrr}_2\text{py})\text{FeCl}]$  (**2**), and c)  $[(\text{pyrr}_2\text{py})\text{Fe}=\text{NAd}]$  (**3**), showing selected atom labeling. Thermal ellipsoids are set at 50% probability and hydrogen atoms have been removed for clarity.

106.21(7)°, N2-Fe1-N3=116.6(2)°) to the nitrogens of the pyrr<sub>2</sub>py ligand. The Fe–N<sub>py</sub> (Fe1–N2=1.867(3) Å) and Fe–N<sub>pyrr</sub> (Fe1–N1=1.910(2) Å) bond distances in **3** are noticeably shorter than those of both **1** and **2** and the iron center deviates from the plane of the pyrr<sub>2</sub>py nitrogens by 0.52 Å. In all, this is consistent with a low-spin, metal-centered, oxidized iron ion. Unlike the few structurally characterized Fe<sup>IV</sup> imides which have nearly linear Fe–N<sub>imide</sub>–C<sub>ipso</sub> angles, the angle measured for **3** is significantly more acute (Fe1–N3–C16=140.5(3)°). Furthermore, the Fe–N<sub>imide</sub> bond length (Fe1–N3=1.640(4) Å) is slightly longer when compared to the range of 1.618–1.635 Å for tetrahedral Fe<sup>IV</sup> imide complexes,<sup>[6a–c]</sup> but significantly shorter than an octahedral Fe<sup>IV</sup> imide distance of 1.73 Å determined from EXAFS measurements by Que et al.<sup>[6d]</sup> Both the <sup>1</sup>H and <sup>13</sup>C NMR spectra of **3** recorded at room temperature in C<sub>6</sub>D<sub>6</sub> exhibit sharp resonance signals with chemical shifts in the normal diamagnetic range, spanning  $\delta$  = 1.14–6.64 ppm and  $\delta$  = 28.84–159.90 ppm, respectively. The number of resonance signals is in accord with a C<sub>s</sub> symmetric species, and thus is consistent with the solid-state structure being retained in solution. SQUID magnetization measurements were also performed to establish the *S* = 0 state of **3**.<sup>[9]</sup>

Given that Fe<sup>IV</sup> imide complexes have been shown to have intermediate spin states,<sup>[6]</sup> and that Fe<sup>III</sup> metal centers antiferromagnetically coupled to an imide-based radical have been reported by the research groups of Chirik<sup>[11]</sup> and Betley,<sup>[12]</sup> we collected zero-field <sup>57</sup>Fe Mössbauer spectra at 77 K on complexes **1–3** (Figure 2) in an attempt to further authenticate the iron oxidation state. Accordingly, complexes **1**, **2**, and **3** produced quadrupole doublets with isomer shifts,  $\delta$ , of +0.86(1), +0.39(1), and –0.09(1) mm s<sup>–1</sup>, and quadrupole splitting values,  $\Delta E_Q$ , of 1.12(1), 2.38(1), and 2.78(1) mm s<sup>–1</sup>, respectively. As the local geometry at the iron center experiences minimal change upon one- and two-electron oxidations of complex **1**, the consistent change in isomer shift of approximately 0.48 mm s<sup>–1</sup> indicates that iron centers in complexes **1–3** are each indeed in different oxidation states. Furthermore, the slightly negative  $\delta$  value detected for **3** is comparable to that of Lee's tetranuclear Fe<sup>IV</sup> imide cluster ( $\delta$  = –0.17 mm s<sup>–1</sup>)<sup>[6a]</sup> and Que's octahedral Fe<sup>IV</sup> imide complex ( $\delta$  = +0.02 mm s<sup>–1</sup>).<sup>[6d]</sup>

As a result of the unique electronic configuration of the Fe<sup>IV</sup> imide complex, complex **3** was further examined by density functional theory (DFT) calculations. A model complex substituting the two *tert*-butyl groups at the 3-position of the pyrrol rings with hydrogen atoms in a spin singlet state (*S* = 0) accurately reproduces the metrical parameters determined by X-ray analysis.<sup>[9]</sup> The subsequent analysis of frontier molecular orbitals (MOs) reveals the electronic configuration of the iron center and the details of bonding in the *cis*-divacant geometry. Within the chosen coordinate system, d<sub>xy</sub> and d<sub>xz</sub> orbitals are doubly occupied MOs, whereas d<sub>yz</sub>, d<sub>z<sup>2</sup></sub>, and d<sub>x<sup>2</sup>–y<sup>2</sup></sub> orbitals become unoccupied (Figure 3). This configuration is consistent with a low-spin Fe<sup>IV</sup> center. The d<sub>x<sup>2</sup>–y<sup>2</sup></sub> and d<sub>z<sup>2</sup></sub> orbitals are substantially destabilized because of strong  $\sigma$ -donation from the three pyrr<sub>2</sub>py nitrogens and the N<sub>imide</sub>, respectively. The d<sub>xz</sub> and d<sub>yz</sub> orbitals show prevailing  $\pi^*$  antibonding character to the N<sub>imide</sub> but

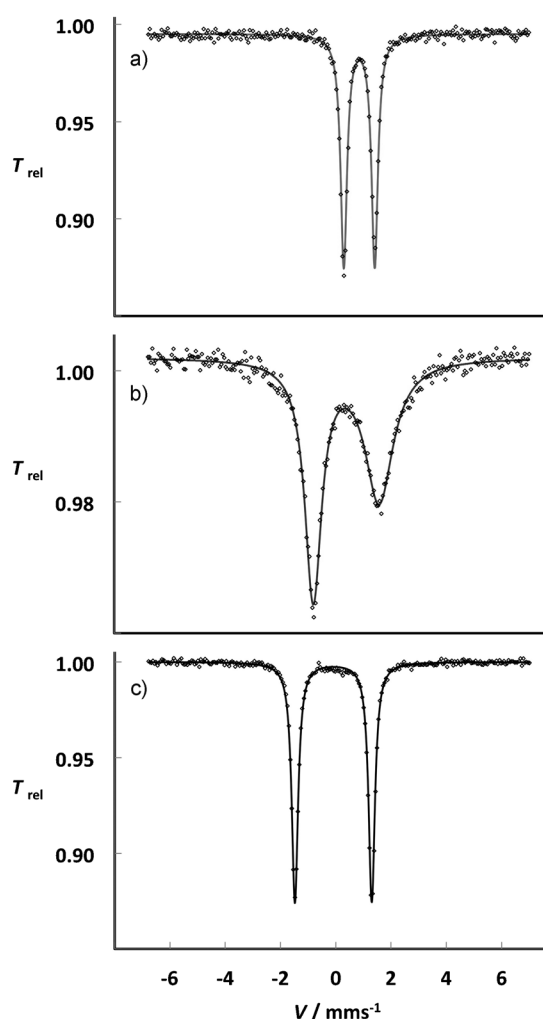


**Figure 2.** Zero-field <sup>57</sup>Fe Mössbauer spectra of a) [(pyrr<sub>2</sub>py)Fe(OEt<sub>2</sub>)] (**1**), b) [(pyrr<sub>2</sub>py)FeCl] (**2**), and c) [(pyrr<sub>2</sub>py)Fe=NAd] (**3**) recorded at 77 K (see text for simulation parameters). *T<sub>rel</sub>* = relative transmission. Open symbols represent experimental data and solid lines represent fitted data.

experience differing degrees of destabilization, resulting in a bent imido group (Fe1–N3–C16: calculated angle = 142.0°, experimental = 140.5°). General considerations indicate that the more acute is the Fe–N–C angle, the more double-bond character the Fe–N<sub>imide</sub> bond has. In the case of **3** this is supported by Loewdin and Mayer population analysis indicating an Fe–N<sub>imide</sub> bond order of 2.18 and 2.02, respectively. Finally, the d<sub>xy</sub> orbital is essentially nonbonding and thus is the lowest energy *d*-orbital.

The accuracy of the calculated *S* = 0 electronic structure for **3** was further validated by calculating Mössbauer parameters. Both the calculated isomer shift (–0.14 mm s<sup>–1</sup>) and quadrupole splitting (–3.14 mm s<sup>–1</sup>) are in good agreement with the experimentally obtained values. Interestingly, the largest component of electric field gradient (EFG)<sup>[13]</sup> *V<sub>zz</sub>* = –1.85 lies not along Fe–N<sub>imide</sub> bond as one might expect, but approximately along the Fe–N<sub>pyrr<sub>2</sub>py</sub> vector.<sup>[9]</sup> We calculated an *S* = 1 state for the model of **3** as well. Both the calculated

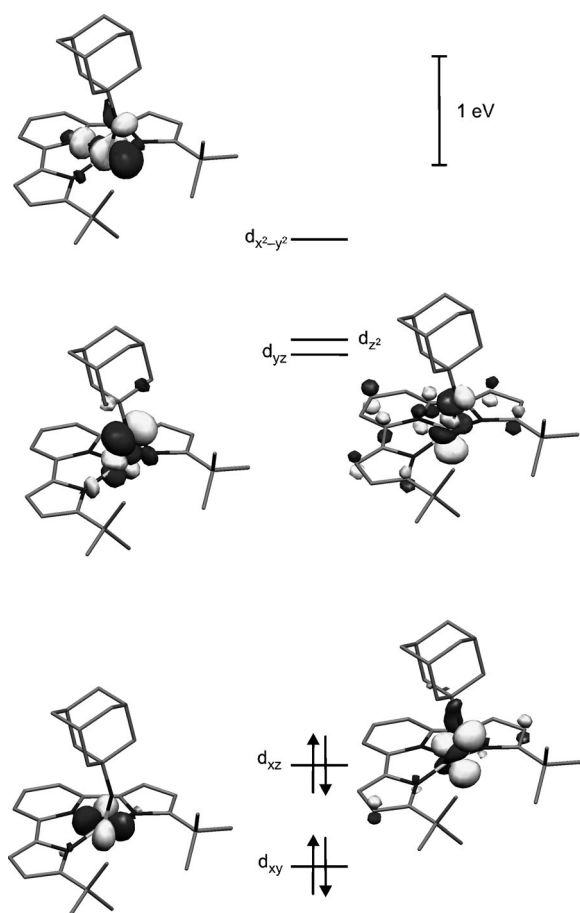


**Figure 3.** Frontier metal-based molecular orbitals for a model complex of **3** ( $S=0$ ) obtained from spin-unrestricted B3LYP-DFT calculations. The  $x$  and  $y$ -axes are placed in the approximate plane of the pyr<sub>2</sub>py ligand and the  $z$ -axis is approximately along the Fe–N<sub>imide</sub> bond vector. Kohn–Sham orbitals are shown.

geometry and the Mössbauer parameters for the  $S=1$  state do not match the experimentally obtained data,<sup>[9]</sup> which supports strongly an  $S=0$  state for complex **3**.

Finally, we checked the influence of the *tert*-butyl groups at the 5-position of the pyrrolyl rings on the coordination geometry. Thus, all four *tert*-butyl groups of the pyr<sub>2</sub>py ligand were replaced with hydrogens, and the geometry of the truncated complex was optimized for an  $S=0$  state. To our surprise, in the absence of bulky *tert*-butyl groups and the geometrical flexibility of the molecule, the unusual *cis*-divacant coordination geometry was preserved.<sup>[9]</sup> Multiple attempts to obtain any other geometry by varying the starting point all converged to the same structure with  $\tau_4=0.62$ .<sup>[10]</sup> Thus, although two bulky *tert*-butyl groups at the 5-position of the pyrrolyl rings prevent formation of a planar geometry for **3**, the electronic factors seem to be a driving force for formation of *cis*-divacant geometry.

Considering all data, we believe that complex **3** can be best described as a low-spin Fe<sup>IV</sup> imide species ( $S=0$ ). It should also be noted that the direct oxidation of Fe<sup>II</sup> centers by organic substrates to generate an Fe<sup>IV</sup> imide derivative is a rare phenomenon<sup>[6d]</sup> and typically requires low-valent Fe<sup>0</sup> or

Fe<sup>I</sup> synthons as two-electron reductants.<sup>[6b,c,11,14]</sup> Furthermore the geometry and low-spin configuration of **3** is unprecedented, indicating that the pyr<sub>2</sub>py pincer ligand is a robust, strongly electron-donating, and most notably, redox-innocent ligand and scaffold that enforces an unusual geometry.

In conclusion, we have described the meridional coordination of the bis(pyrrolyl)pyridine ligand (pyr<sub>2</sub>py) to a series of iron complexes ranging from Fe<sup>II</sup>–Fe<sup>IV</sup>. In all cases, the unusual trigonal pyramidal to *cis*-divacant octahedral geometry is maintained by the pyr<sub>2</sub>py ligand. Additionally, we have shown that the direct two-electron oxidation of [(pyr<sub>2</sub>py)Fe(OEt<sub>2</sub>)] (**1**) results in the unique, and high-yield synthesis of an Fe<sup>IV</sup> imide complex [(pyr<sub>2</sub>py)Fe=NAd] (**3**) which has an  $S=0$  state. Calculations also indicate that removal of the *tert*-butyl substituents from the pyr<sub>2</sub>py ligand results in retention of the *cis*-divacant geometry. This opens exciting perspectives in tuning the reactivity of the complex by replacing bulky *tert*-butyl groups with smaller substituents, thus rendering the Fe<sup>IV</sup> center more available for coordination by substrate molecules. Constraining the Fe<sup>IV</sup> center to this unusual geometry allows for the stabilization of a terminally bound imido ligand that does not have the expected radical character at the imide nitrogen atom. This opens the possibility to stabilize high-valent metal centers having metal–ligand multiple bonds by manipulating their geometry and coordination number.

Received: July 13, 2014

Revised: August 26, 2014

Published online: October 19, 2014

**Keywords:** density functional calculations · iron · magnetic properties · Mössbauer spectroscopy · N ligands

- [1] a) J. T. Groves, *J. Inorg. Biochem.* **2006**, *100*, 434; b) J. Hohenberger, K. Ray, K. Meyer, *Nat. Commun.* **2012**, *3*, 720; c) C. Krebs, D. Galonić Fujimori, C. T. Walsh, J. M. Bollinger, *Acc. Chem. Res.* **2007**, *40*, 484.
- [2] M. Sono, M. P. Roach, E. D. Coulter, J. H. Dawson, *Chem. Rev.* **1996**, *96*, 2841.
- [3] E. W. Svastits, J. H. Dawson, R. Breslow, S. H. Gellman, *J. Am. Chem. Soc.* **1985**, *107*, 6427.
- [4] a) S. A. Cramer, D. M. Jenkins, *J. Am. Chem. Soc.* **2011**, *133*, 19342; b) E. Gouré, F. Avenier, P. Dubourdeaux, O. Sénéque, F. Albrieux, C. Lebrun, M. Clémancey, P. Maldivi, J.-M. Latour, *Angew. Chem. Int. Ed.* **2014**, *53*, 1580; *Angew. Chem.* **2014**, *126*, 1606.
- [5] a) J. U. Rohde, J. H. In, M. H. Lim, W. W. Brennessel, M. R. Bukowski, A. Stubna, E. Munck, W. Nam, L. Que, *Science* **2003**, *299*, 1037; b) E. J. Klinker, J. Kaizer, W. W. Brennessel, N. L. Woodrum, C. J. Cramer, L. Que, *Angew. Chem. Int. Ed.* **2005**, *44*, 3690; *Angew. Chem.* **2005**, *117*, 3756; c) A. Thibon, J. England, M. Martinho, V. G. Young, J. R. Frisch, R. Guillot, J. J. Girerd, E. Munck, L. Que, F. Banse, *Angew. Chem. Int. Ed.* **2008**, *47*, 7064; *Angew. Chem.* **2008**, *120*, 7172; d) J. England, Y. S. Guo, E. R. Farquhar, V. G. Young, E. Munck, L. Que, *J. Am. Chem. Soc.* **2010**, *132*, 8635; e) D. C. Lacy, R. Gupta, K. L. Stone, J. Greaves, J. W. Ziller, M. P. Hendrich, A. S. Borovik, *J. Am. Chem. Soc.* **2010**, *132*, 12188.
- [6] a) A. K. Verma, T. N. Nazif, C. Achim, S. C. Lee, *J. Am. Chem. Soc.* **2000**, *122*, 11013; b) C. M. Thomas, N. P. Mankad, J. C. Peters, *J. Am. Chem. Soc.* **2006**, *128*, 4956; c) I. Nieto, F. Ding,



- R. P. Bontchev, H. Wang, J. M. Smith, *J. Am. Chem. Soc.* **2008**, *130*, 2716; d) E. J. Klinker, T. A. Jackson, M. P. Jensen, A. Stubna, G. Juhász, E. L. Bominaar, E. Münck, L. Que, *Angew. Chem. Int. Ed.* **2006**, *45*, 7394; *Angew. Chem.* **2006**, *118*, 7554; e) For a recently reported three-coordinate Fe<sup>IV</sup> bis-imide, see: H. Zhang, Z. Ouyang, Y. Liu, Q. Zhang, L. Wang, L. Deng, *Angew. Chem. Int. Ed.* **2014**, *53*, 8432; *Angew. Chem.* **2014**, *126*, 8572.
- [7] J. M. Mayer, *Comments Inorg. Chem.* **1988**, *8*, 125.
- [8] N. Komine, R. W. Buell, C.-H. Chen, A. K. Hui, M. Pink, K. G. Caulton, *Inorg. Chem.* **2014**, *53*, 1361.
- [9] See Supporting Information for details. CCDC-1001461, 1001462, and 1001463 contain the supplementary crystallographic data for this paper. These data can be obtained free of charge from The Cambridge Crystallographic Data Centre via [www.ccdc.cam.ac.uk/data\\_request/cif](http://www.ccdc.cam.ac.uk/data_request/cif).
- [10] a)  $\tau_4$  is defined as  $(360 - (A + B))/141$ , with  $A$  and  $B$  being the two largest angles of the four-coordinate complex, where  $\tau_4 = 0$  for square planar and  $\tau_4 = 1$  for tetrahedral; b) L. Yang, D. R. Powell, R. P. Houser, *Dalton Trans.* **2007**, 955.
- [11] a) S. C. Bart, E. Lobkovsky, E. Bill, P. J. Chirik, *J. Am. Chem. Soc.* **2006**, *128*, 5302; b) A. C. Bowman, C. Milsman, E. Bill, Z. R. Turner, E. Lobkovsky, S. DeBeer, K. Wieghardt, P. J. Chirik, *J. Am. Chem. Soc.* **2011**, *133*, 17353.
- [12] a) E. R. King, E. T. Hennessy, T. A. Betley, *J. Am. Chem. Soc.* **2011**, *133*, 4917; b) E. T. Hennessy, T. A. Betley, *Science* **2013**, *340*, 591; c) E. T. Hennessy, R. Y. Liu, D. A. Iovan, R. A. Duncan, T. A. Betley, *Chem. Sci.* **2014**, *5*, 1526.
- [13] a) M. M. Khusniyarov, E. Bill, T. Weyhermüller, E. Bothe, K. Harms, J. Sundermeyer, K. Wieghardt, *Chem. Eur. J.* **2008**, *14*, 7608; b) M. M. Khusniyarov, T. Weyhermüller, E. Bill, K. Wieghardt, *J. Am. Chem. Soc.* **2009**, *131*, 1208.
- [14] a) S. D. Brown, T. A. Betley, J. C. Peters, *J. Am. Chem. Soc.* **2003**, *125*, 322; b) T. A. Betley, J. C. Peters, *J. Am. Chem. Soc.* **2003**, *125*, 10782; c) S. D. Brown, J. C. Peters, *J. Am. Chem. Soc.* **2005**, *127*, 1913; d) C. C. Lu, C. T. Saouma, M. W. Day, J. C. Peters, *J. Am. Chem. Soc.* **2007**, *129*, 4; e) M.-E. Moret, J. C. Peters, *Angew. Chem. Int. Ed.* **2011**, *50*, 2063; *Angew. Chem.* **2011**, *123*, 2111; f) R. E. Cowley, N. J. DeYonker, N. A. Eckert, T. R. Cundari, S. DeBeer, E. Bill, X. Ottenwaelde, C. Flaschenriem, P. L. Holland, *Inorg. Chem.* **2010**, *49*, 6172; g) R. E. Cowley, P. L. Holland, *Inorg. Chem.* **2012**, *51*, 8352; h) C. Ni, J. C. Fetting, G. J. Long, M. Brynda, P. P. Power, *Chem. Commun.* **2008**, 6045; i) S. Kuppuswamy, T. M. Powers, B. M. Johnson, M. W. Bezpalko, C. K. Brozek, B. M. Foxman, L. A. Berben, C. M. Thomas, *Inorg. Chem.* **2013**, *52*, 4802.